Carbohydrate Polymers 117 (2015) 537–542

Contents lists available at ScienceDirect

Carbohydrate Polymers

journal homepage: www.elsevier.com/locate/carbpol

Carboxymethylagarose-AuNPs generated through green route for selective detection of Hg^{2+} in aqueous medium with a blue shift

Jai Prakash Chaudhary[a,b], Anshu Kumar[b,c], Parimal Paul[b,c,*], Ramavatar Meena[a,b,*]

[a] Scale-Up & Process Engineering Unit, CSIR—Central Salt and Marine Chemicals Research Institute, G. B. Marg, Bhavnagar 364 002, India
[b] Academy of Scientific & Innovative Research-Central Salt and Marine Chemicals Research Institute, G. B. Marg, Bhavnagar 364 002, India
[c] Analytical Discipline and Centralized Instrument Facility, CSIR Central Salt & Marine Chemicals Research Institute, Bhavnagar 364 002, India

ARTICLE INFO

Article history:
Received 6 July 2014
Received in revised form 9 October 2014
Accepted 10 October 2014
Available online 18 October 2014

Keywords:
CMA-AuNPs
Green process
Blue shift
Amalgam
Mercury sensor

ABSTRACT

We report here a facile, rapid, cost-effective method *via* a green route for the selective detection of Hg^{2+} in aqueous media. In this study carboxymethylagarose (CMA) is used to generate gold nanoparticles and subsequently to act as a stabilizer for the CMA-functionalized gold nanoparticles (CMA-AuNPs). The resulting CMA-AuNPs was characterized by UV–visible, X-ray diffraction, transmission electron microscopy (TEM), dynamic light scattering (DLS), atomic force microscopy (AFM) and zeta potential measurements. Zeta potential value (∼ −73 mv) of CMA-AuNPs in the aqueous medium shows its higher stability. When CMA-AuNPs were exposed to an aqueous Hg^{2+}, a blue shift for its localized surface plasmon resonance absorbance (LSPR) band is observed along with significant colour change of the solution. The probe enables to detect Hg^{2+} in the range of 0.01–100 ppm even in spiked lake water samples. This study offers a sustainable and eco-friendly route for selective detection of Hg^{2+} in aqueous solution and may find potential application towards water purification.

1. Introduction

Mercury, a well-known highly toxic and dangerous environmental pollutant routinely released from small scale gold mining, coal-based power plants, metal refining plants, oceanic and volcanic emissions *etc*. The long atmospheric residence time of Hg (0) vapour and its oxidation to soluble inorganic Hg^{2+} provide a pathway for contaminating surrounding environment including water and soil. Bio-organism like bacteria living in an aqueous environments transform inorganic Hg^{2+} into methyl mercury, which is a powerful neurotoxin that concentrates through the food chain in the tissues of fishes and marine mammals. Subsequent ingestion of methyl mercury by humans from sea-food and other dietary sources is connected to the many serious problems such as sensory, motor, and cognitive disorders. The higher levels of Hg^{2+} can be dangerous to the brain, heart, lungs *etc*. of humans. According to an estimate the total mercury released into the environment reaches to ∼7500 t/year (Hoyle & Handy, 2005). The United Nations ratified a new Convention on Mercury Control on January 19, 2013, following multinational dialogues that began on January 2013. Because toxic mercury ion contamination normally accumulates in existing organisms and slowly progresses over time, therefore timely detection of low concentrations of Hg in environmental water is a key issue for the researchers. Thus it is very important to develop an extremely high sensitivity, cost-effective and bio-based Hg^{2+} sensor that can provide real-time determination of Hg^{2+} levels in the environment, water, and food (Darbha, Ray, & Ray, 2007). A great effort has been exerted to detect Hg^{2+} using various detection techniques, including optical spectroscopy (Jiang et al., 2012; Lim, Escobedo, Lowry, Xu, & Strongin, 2010; Rusin et al., 2003; Wang et al., 2005; Wang, Heon Lee, & Lu, 2008), electrochemical methods (Liu, Nie, Jiang, Shen, & Yu, 2009; Spătaru, Sarada, Popa, Tryk, & Fujishima, 2001), high-performance liquid chromatography (Chen, Chen, Jin, & Wei, 2009; Lu, Zu, & Yam, 2007), inductively coupled plasma mass spectrometry, and so forth (Chen et al., 2009; Li et al., 2006). However, most of these techniques require expensive instrumentation and complicated sample preparation in certain cases, which make them inappropriate for point of use applications. To overcome these drawbacks, a variety of colorimetric sensors based on gold nano particles (AuNPs) have been attempted for the simple and rapid detection of Hg^{2+} (Kumar & Paul, 2014; Lee, Ulmann, Han, & Mirkin, 2008; Maity, Kumar, Gunupuru, & Paul, 2014; Xue, Wang, & Liu, 2008; Yu & Tseng, 2008; Zhang, Xu, Yuan, Yang, & Yang, 2011).

* Corresponding authors at: Central Salt and Marine Chemicals Research Institute, G. B. Marg, Bhavnagar 364002, Gujarat, India. Tel.: +91 278 2567760; fax: +91 278 2567562.
E-mail addresses: ppaul@csmcri.org (P. Paul), rmeena@csmcri.org, ramavatar73@yahoo.com (R. Meena).

http://dx.doi.org/10.1016/j.carbpol.2014.10.016
0144-8617/

The utilization of nontoxic chemicals, environmentally benign solvents and renewable materials are some of the key issues that merit important consideration in a green synthesis strategy (Poliakoff & Anastas, 2001; DeSimone, 2002; Raveendran, Fu, & Wallen, 2003). In literature natural polymers like starch and chitosan are reported to stabilize silver nanoparticles (Raveendran et al., 2003; Huang & Yang, 2004b).

Nanoparticles have potential applications in medical diagnosis and therapeutics like detection of genetic disorders by using gold nanoparticles, (Boisselier & Astruc, 2009; Cao, Jin, & Mirkin, 2002; Taton, Mirkin, & Letsinger, 2000) colour-coded fluorescent labelling of cells using semiconductor quantum dots (Chan & Nie, 1998) and drug delivery (Sandhu, McIntosh, Simard, Smith, & Rotello, 2001), are reported in literature. Therefore use of biologically compatible materials for nanoparticles synthesis and stabilization will undoubtedly play a crucial role in this area. In addition, physical properties of gold nanoparticles are actually different from other nano scale particles such as ability to display brilliant colours, which further made them extremely smart objects of study for researches (Dreaden, Alkilany, Huang, Murphy, & El-Sayed, 2012). Biopolymers like chitosan, carboxymethyl chitosan, heparin and hyaluronan are also reported in the literature for synthesis and stabilization of silver and gold nano particles (Huang & Yang, 2004a; Huang & Yang, 2004b; Kemp et al., 2009). Gold nanoparticles in both colloidal solutions and films respond to elemental mercury with blue shifts in localized surface Plasmon resonance (LSPR) wavelength (Chen et al., 2009; Jiang et al., 2012; Li et al., 2006; Lim et al., 2010; Liu et al., 2009; Lu et al., 2007; Rusin et al., 2003; Spătaru et al., 2001; Zhang et al., 2011). The above reports indicates that there are no reports on the synthesis and stabilization of gold nanoparticles (AuNPs) using carboxymethylagarose.

The present study described the use of carboxymethylagarose (CMA) for the synthesis and stabilization of gold nanoparticles for the first time. Subsequently, CMA-AuNPs was successfully used as colorimetric probe for selective detection of Hg^{2+} ions at room temperature in neutral aqueous medium.

2. Experimental

2.1. Materials

Carboxymethylagarose (CMA) was synthesized by the process described in our previous work (Chaudhary, Kondaveeti, Gupta, Prasad, & Meena, 2014), using agarose extracted from *Gracilaria dura* as described in our previous work (Meena et al., 2014). Hydrogen tetrachloroaurate ($HAuCl_4{\cdot}3H_2O$), $NaBH_4$, mercuric perchlorate, lead perchlorate, cadmium perchlorate, manganese perchlorate, silver perchlorate, nickel perchlorate and copper perchlorate, zinc perchlorate, chromium perchlorate, were purchased from Sigma-Aldrich and used without further purification. HNO_3 was purchased from S. D. Fine, India.

2.2. Characterizations

UV–visible absorption spectra were recorded on Varian Cary-500 (Shimadzu UV 3600) spectrophotometer. Transmission electron microscope (TEM) images were recorded on a HR-TEM (JEOL GEM 2100) instrument operated at an accelerated voltage of 200 kV. Powder XRD was recorded on a model Empyrean powder XRD (Cu-*K*α radiation) supplied by PAN analytical Netherland. AFM analysis was carried out using NTEGRA, TS-150 instrument by Table stable Ltd., USA. DLS measurement was carried out using Malvern instrument UK at a scattered angle of 90° at 30 °C. The incident light was the 488 nm of Argon laser GSL 3110. Surface charge on the CMA-AuNPs was monitored by zeta potential measurements using Malvern Instruments, U.K.

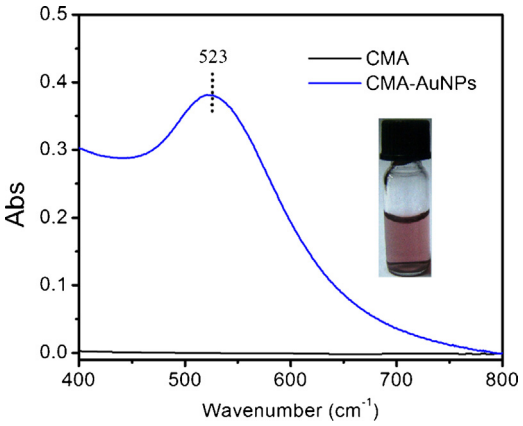

Fig. 1. UV–visible absorption spectra of CMA-AuNPs.

2.3. Preparation of CMA-AuNPs

In a typical synthetic procedure, 0.5 mL of 0.01 M $HAuCl_4{\cdot}3H_2O$ and 0.5 mL of 0.1% w/v CMA in water were added to 14 mL of deionized H_2O under stirring at room temperature. Then 0.5 mL freshly prepared 0.1 M $NaBH_4$ was added under stirring, and the colour of solution was changed from colourless to purple, stirring was stopped, and whole solution was washed with methanol to remove the excess $NaBH_4$. The resulting CMA-AuNPs were dispersed in Milli-Q water and left undisturbed for 12 h. Finally whole solution was stored in refrigerator for further study.

3. Results and discussion

3.1. Selectivity of metal ions with CMA-AuNPs

Fig. 1 shows the UV spectra of the CMA and CMA-AuNPs. The LSPR absorption maximum observed at 523 nm confirmed the formation of CMA-AuNPs (Radhakumary & Sreenivasan, 2011).The size of CMA-AuNPs obtained in the present study ranges from 5 to 7 nm and exhibited an absorption maximum at 523 nm and was in good agreement with those reported in literature (Huang & Yang, 2004b; Pal, Esumi, & Pal, 2005; Watthanaphanit, Panomsuwan, & Saito, 2014). To investigate the interaction of different metal ions with CMA-AuNPs, 100 ppm aqueous solutions of metal ions (*e.g.* Hg^{2+}, Pb^{2+}, Cd^{2+}, Ag^{+}, Ni^{2+}, Cu^{2+}, Zn^{2+}, Co^{2+}, Fe^{3+}, and Cr^{3+}) were prepared from their respective salts. The absorption maxima of the CMA-AuNPs before and after addition of 100 ppm of each metal ions solution was recorded (Fig. 2A and B). The absorption maxima of CMA-AuNPs did not show any significant blue shift on interacting with all the cations except Hg^{2+} (obtained blue shift from 523 nm to 512 nm) revealed selective interaction with mercury ions (Fig. 2A and B). Interestingly on the addition of 100 ppm of Ag^{+} ions in the CMA-AuNPs solution causes a slight red shift in LSPR maxima was obtained (Fig. 2A). These results revealed that CMA-AuNPs prepared in this study had a high selectivity towards Hg^{2+} ions and could be employed as colorimetric probe for Hg^{2+}.

3.2. Optimization for detection of Hg^{2+}

Effect of pH of aqueous media on the detection capability of this probe is shown in Fig. S1. This study revealed that this probe is highly suitable for aqueous media with pH 7 as maximum blue shifting of 11 nm (from 523 nm to 512 nm) was observed. Furthermore, To optimized the incubation time for interaction of Hg^{2+}

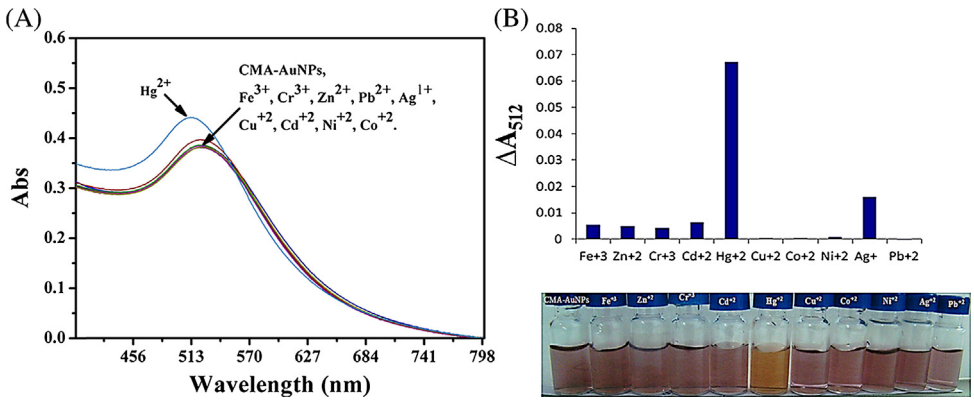

Fig. 2. Absorption spectra of (A) CMA-AuNPs with 100 ppm solution of different metal ions, and (B) selectivity of CMA-AuNPs to Hg^{2+} and other metal ions.

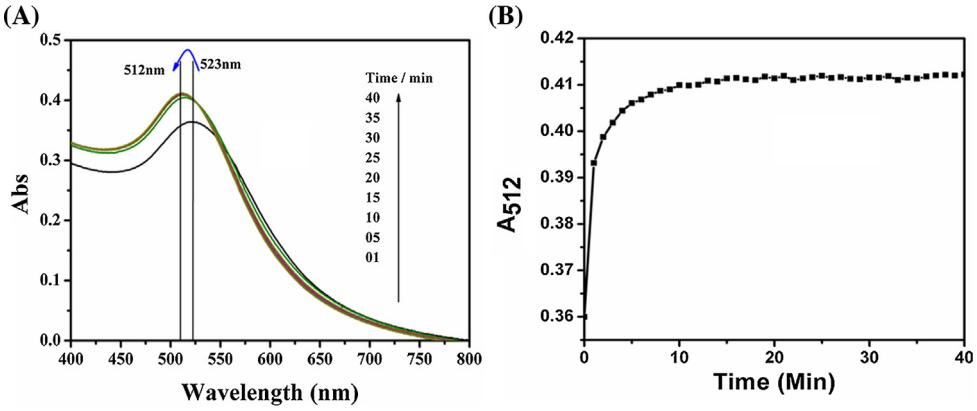

Fig. 3. Time course measurements of (A) UV–visible extinction spectra for CMA-AuNPs after the addition of Hg^{2+} (100 ppm), and (B) A_{512} for CMA-AuNPs after the addition of Hg^{+2} (100 ppm).

ions with CMA-AuNPs, sevreal experiments were carried out using 100 ppm Hg^{2+} solution in CMA-AuNPs (Fig. 3A and B). The blue shift in LSPR band increased (from 523 nm to 512 nm) when increasing the incubation time at room temperature up to 10 min and got steady beyoned this time period. This result revealed that 10 min duration is sufficient for the optimum interaction of Hg^{2+} with CMA-AuNPs. This revealed that CMA-functionalized AuNPs synthesized in this study rquired only 10 min for the complete interaction with Hg^{2+}.

3.3. Sensitivity of Hg^{2+}

To investigate the senitivity of CMA-AuNPs towards Hg^{2+}, 0.01, 0.1, 1.0, 10 and100 ppm solutions of Hg^{2+} were prepared and added to CMA-AuNPs probe and LSPR absorption spectra were recorded under identical conditions (Fig. 4). The greatest blue shift in the LSPR band of 11 nm (from 523 to 512 nm) was obtained in the range of 0.1–100 ppm Hg^{2+} solution and beyond this concentration no shifting was observed may be due to the saturated of CMA-AuNPs with Hg^{2+}, however our probe exhibited a least blue shift of 6 nm (from 523–517 nm) with 0.01 ppm of Hg^{2+} (Fig. 4 and Fig. S2). The results obtained were in good agreement with those of reported in the literature for chitosan-functionalized gold nanoparticles (Radhakumary & Sreenivasan, 2011). The colour change of CMA-AuNPs probe from purple to orange after addition of Hg^{2+} further confirmed the formation of amalgam (Au–Hg). This result confirmed that CMA-AuNPs probe can selectively detects Hg^{2+} in the aqueous solution in the range of 0.01 to 100 ppm. Each set of experiments was carried out in triplicate to confirm the precision and recovery of the probe and similar results within the maximum error of 1–2% were obtained.

3.4. Mechanistic study

Scheme 1 shows a mechanism of the synthesis of CMA-AuNPs and detection of Hg^{2+}, which self-evidentiary that the synthesis route is a simple, green and cost-effective. Carboxymethylagarose

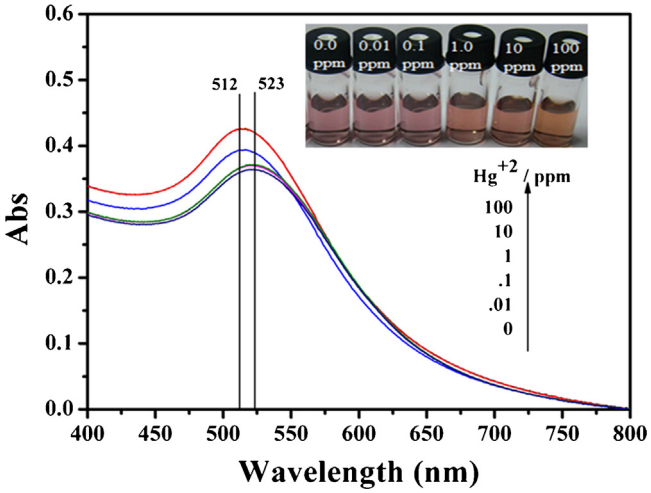

Fig. 4. Absorption spectra of CMA-AuNPs showing blue shift on interacting with different concentrations of Hg^{+2} standard. (For interpretation of the references to color in this figure legend, the reader is referred to the web version of this article.)

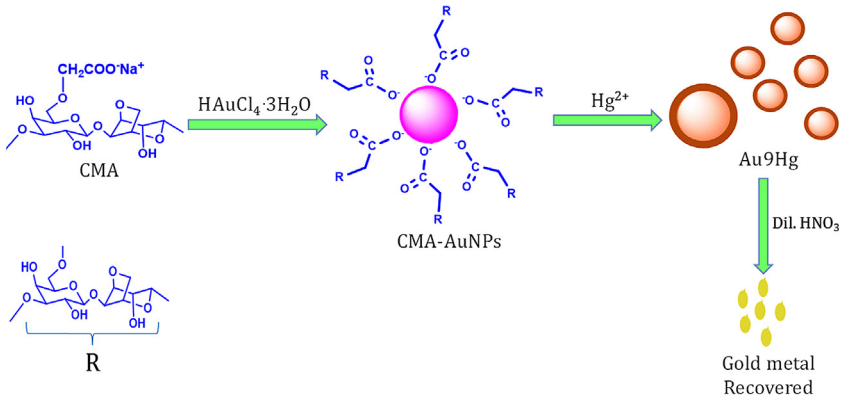

Scheme 1. Plausible mechanism of the synthesis of CMA-AuNPs and detection of Hg^{2+}.

(CMA) was used for the synthesis and stabilization of gold nanoparticles and was used successfully for selective detection of Hg^{2+} ion in aqueous medium. The obtained CMA-AuNPs were highly stable (zeta potential, $\zeta \equiv -73 \pm 3$) and can be stored under refrigeration conditions for more than 5 months. The carboxylate ions ($-COO^-$) on CMA backbone may have strong interactions with gold nanoparticles and formed a polymeric layer on the surface of nanoparticles, which may protect AuNPs against metal salt-induced aggregation (Wei, Qi, Tan, Liu, & Wang, 2010). The similar observation has been reported in the literature for reducing agent such as citrate in the formation of Au–Hg amalgam (Kumar & Paul, 2014).

In the present study perhaps carboxylate ions of CMA coated onto the surface of CMA-AuNPs, act as a reducing agent to form Au–Hg. The change in UV absorption spectrum of CMA after addition of Hg^{2+} also revealed the interaction between CMA and Hg^{2+}. On addition of Hg^{2+} in CMA solution the absorption intensity was enhanced (Fig. S3), indicating the formation of CMA-Hg^{2+}. The formation of Au–Hg amalgam was further analysed by TEM and XRD, which confirmed that the proposed process for Hg^{2+} detection involved core-etching process of CMA-AuNPs.

Fig. 5 shows the TEM images of the CMA-AuNPs before and after addition of 10 ppm and 100 ppm of Hg^{2+}. Fig. 5A shows that the diameter of CMA-AuNPs was ranged between 5 and 7 nm. Fig. 5B,C and Fig. S4 showed that the addition of Hg^{2+} in CMA-AuNPs probe results in blue shift (from 523 nm to 512 nm) in LSPR absorption spectra due to core etching of AuNPs in form of amalgam (diameter range from 2.3 to 5 nm) (Ho-Cheng, Tzu-Heng, Wei-Lung, & Che-Hsin, 2012). Fig. 5D shows the diffraction pattern of CMA-AuNPs

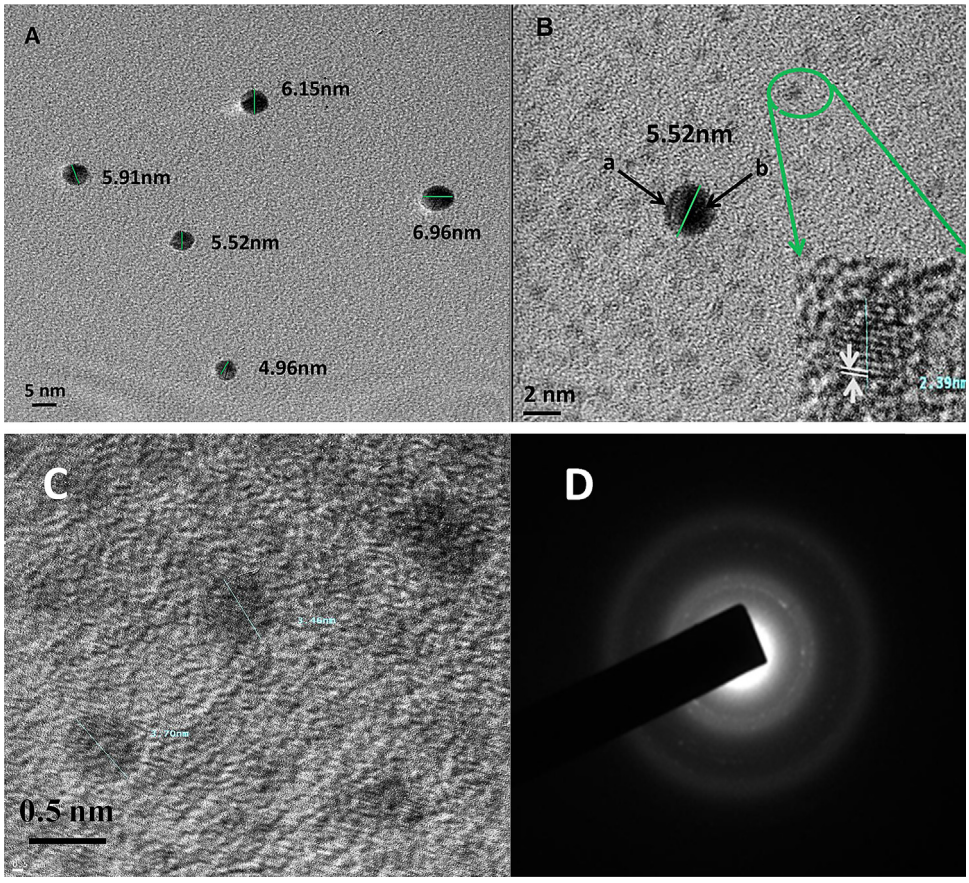

Fig. 5. TEM images of (A) CMA-AuNPs (B) CMA-AuNPs with 10 ppm Hg^{2+} (C) lattice fringes of CMA-AuNPs with 10 ppm Hg^{2+} (D) diffraction pattern of B.

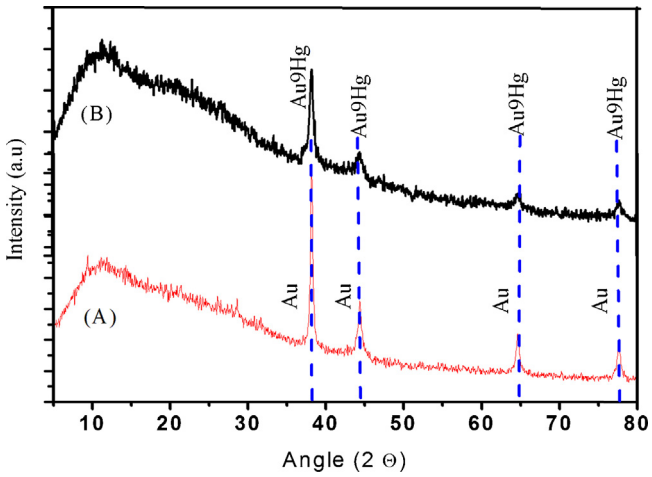

Fig. 6. XRD pattern of (A) CMA-AuNPs (B) CMA-AuNPs with 10 ppm Hg^{2+}.

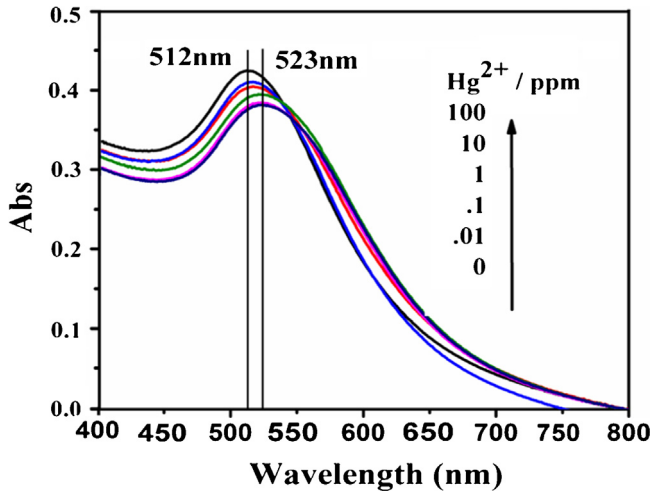

Fig. 7. UV absorption spectra of lake water sample spiked with different (0.01 to 100 ppm) concentration of Hg^{2+} ions.

Table 1
Effect of Hg^{2+} on zeta potential value and average particle size of CMA-AuNPs.

Sample	Zeta potential (mv)	Average particle diameter from TEM (nm)
CMA-AuNPs	−73 ± 3	6.15
CMA-AuNPs-Hg^{2+}−1 ppm	−52 ± 2	5.15, 3.69
CMA-AuNPs-Hg^{2+}−10 ppm	−49.5 ± 2	5.35, 2.69
CMA-AuNPs-Hg^{2+}−100 ppm	−50 ± 2	5.10, 2.39

after interaction with 10 ppm of Hg^{+2}. Size of the CMA-AuNPs has been further confirmed by AFM and DLS analysis as shown in Figs. S5 and S6. The AFM (Fig. S5) and DLS (Fig. S6) results are in good agreement with that of TEM results (Fig. 5). Liu, Chen, Wang, Qu, Chen, and Wang (2013) has also reported similar decreament in the diameter in case of the etching of AuNPs by the co-work of Cu^{2+} and $S_2O_3^{2-}$. TEM image as given in Fig. 5B confirmed that there were different region in a single CMA-AuNP. Since the electron densities of the metals are reflected in the contrast images (Manivannan & Ramaraj, 2009). Fig. 5B shows two part in a CMA-AuNPs, part (a) shows less contrast image it means less electron densities of the AuNP and part (b) shows more contrast image it means high electron densities of the AuNPs. Alternatively, as in the core etching mechanism mentioned above, Hg^{2+} can also tend to split the original synthesiszed CMA-AuNPs into smaller ones as shown in Fig. S4.

Fig. 6 shows X-ray diffraction pattren of CMA-AuNPs before and after addition of Hg^{2+}. The X-ray diffraction pattren of CMA-AuNPs shows peaks at 38.2054°, 44.4015°, 64.6419°, 77.6333°, which corresponds to the (1 1 1), (2 0 0), (2 2 0) and (3 1 1) Au cubic reflections (JCPDS 04-006-2588), respectively. CMA-AuNPs after interaction with Hg^{2+}, no characteristic peaks of Hg^{2+} was obtained, however a slight shift in 2θ peak (~0.10) was observed. This result revealed the formation of Au–Hg alloy with ratio of 9: 1. The similar results has been reported in the literature (JCPDS no. 00-046-1412).

The zeta potential (ζ) of a particle is the overall charge that particle acquires in a particular medium. Table 1 showed zeta potential value of CMA-AuNPs before and after interacton with 1.0, 10 and 100 ppm Hg^{2+}. The excellent Zeta potential (ζ) value (-73 ± 3) of CMA-AuNPs indicates higher stability of gold nanparticles in the persent study. The value of Zeta potential of AuNPs changed significantly from -73 ± 3 to -52 ± 2 after addtion of 1.0 ppm mercury solution, however no significant effect of Hg^{2+} concentration was observed beyoned 1 ppm (Table 1). This could be explained on the basis of decreasing size of CMA-AuNPs after addition of Hg^{2+} followed by ecthing techniques (Table 1).

3.5. Detection of Hg^{2+} in real samples

To investigate LSPR absorption maxima of CMA-AuNPs on interacting with Lake (Gaurishankar Lake, Bhavnagar, Gujarat, India) water were also investigated. Result of this study revealed that LSPR absorption maxima of CMA-AuNPs did not show any blue shift with lake water indicates absence of Hg^{2+} ions in the lake water. When lake water spiked with 10 ppm of Hg^{2+} is added to CMA-AuNPs probe, a blue shift of 5 nm (Fig. 7) is observed which is in agreement with the 5 nm blue shift observed for 10 ppm Hg^{2+} standard (Fig. 4). To check the further accuracy of CMA-AuNPs probe, an another sets of experiments was carried out by spiking lake water with different concentrations (0, 0.01, 0.1, 1, & 100 ppm) of Hg^{2+}, a significant blue shift of 11 nm observed only for the CMA-AuNPs on addition of 100 ppm Hg^{2+} (Fig. 7), which is in good agreement with the 11 nm blue shift observed for 100 ppm Hg^{2+} standard (Fig. 2). This result revealed that present probe (CMA-AuNPs) could be used for the selective detection of Hg^{2+}. If a small quantity of Hg^{2+} as low as 0.01 ppm had been present in the water samples it would have caused a blue shift of 2 nm for the LSPR of CMA-AuNPs. The absorption at 523 nm starts shifted towards blue shift (from 523 to 512 nm) with an increase of Hg^{2+} concentration in lake water over the range 0.01–100 ppm, similar to the results obtained in pure water (Milli-Q water). Results of this study revealed that CMA-AuNPs probe may be suitable for the detection of Hg^{2+} in real samples. To make the protocol more economical gold metal was recovered by using dil HNO_3.

4. Conclusions

Carboxymethylagarose was used for the synthesis and stabilization of AuNPs in aqueous medium. The resulting CMA-AuNPs probe was used successfully for the selective detection of mercury in the real water samples in the range of 0.01 to 100 ppm. CMA-AuNPs probe exhibits a sharp colour change from purple to orange along with blue shift only after interaction with Hg^{2+}, which helps to detect the mercury in water medium. The recovery of gold metal from the final spent solution makes this process and probe cost-effective. The process is simple and does not involved complex reaction steps and costly chemicals, The results of this study shows that the CMA-AuNPs probe have excellent selectivity to Hg^{2+} over

all other cations (Pb^{2+}, Cd^{2+}, Ag^{+}, Ni^{2+}, Cu^{2+}, Zn^{2+}, Co^{2+}, Fe^{3+}, and Cr^{3+}).

Acknowledgement

CSIR-CSMCRI communication no. CSIR-CSMCRI 095/2014. Authors are thankful to DST, New Delhi, and CSIR (CSC0130), New Delhi, India for financial support (SB/EMEQ-052/2013), and to Dr. S.K. Nataraj for his kind support. JPC & AK are also thankful to AcSIR for enrolment in Ph.D. Anshu acknowledges Council of Scientific and Industrial Research (CSIR), New Delhi, for UGC-JRF fellowship. CSIR-CSMCRI also acknowledged for providing infrastructures and analytical facilities.

Appendix A. Supplementary data

Supplementary data associated with this article can be found, in the online version, at http://dx.doi.org/10.1016/j.carbpol.2014.10.016.

References

Boisselier, E., & Astruc, D. (2009). Gold nanoparticles in nanomedicine: Preparations, imaging, diagnostics, therapies and toxicity. *Chemical Society Reviews*, *38*(6), 1759–1782.

Cao, Y. C., Jin, R., & Mirkin, C. A. (2002). Nanoparticles with Raman spectroscopic fingerprints for DNA and RNA detection. *Science*, *297*(5586), 1536–1540.

Chan, W. C. W., & Nie, S. (1998). Quantum dot bioconjugates for ultrasensitive nonisotopic detection. *Science*, *281*(5385), 2016–2018.

Chaudhary, J. P., Kondaveeti, S., Gupta, V., Prasad, K., & Meena, R. (2014). Preparation and functional evaluation of agarose derivatives. *Journal of Applied Polymer Science*, http://dx.doi.org/10.1002/APP.40630

Chen, H., Chen, J., Jin, X., & Wei, D. (2009). Determination of trace mercury species by high performance liquid chromatography–inductively coupled plasma mass spectrometry after cloud point extraction. *Journal of Hazardous Materials*, *172*(2–3), 1282–1287.

Darbha, G. K., Ray, A., & Ray, P. C. (2007). Gold nanoparticle-based miniaturized nanomaterial surface energy transfer probe for rapid and ultrasensitive detection of mercury in soil, water, and fish. *ACS Nano*, *1*(3), 208–214.

DeSimone, J. M. (2002). Practical approaches to green solvents. *Science*, *297*(5582), 799–803.

Dreaden, E. C., Alkilany, A. M., Huang, X., Murphy, C. J., & El-Sayed, M. A. (2012). The golden age: Gold nanoparticles for biomedicine. *Chemical Society Reviews*, *41*(7), 2740–2779.

Ho-Cheng, L., Tzu-Heng, C., Wei-Lung, T., & Che-Hsin, L. (2012). Novel core etching technique on synthesized gold nanoparticles for colorimetric detection of dopamine biosample. Nano/micro engineered and molecular systems (NEMS). In *Seventh IEEE International Conference* (pp. 665–668).

Hoyle, I., & Handy, R. D. (2005). Dose-dependent inorganic mercury absorption by isolated perfused intestine of rainbow trout, *Oncorhynchus mykiss*, involves both amiloride-sensitive and energy-dependent pathways. *Aquatic Toxicology*, *72*(1–2), 147–159.

Huang, H., & Yang, X. (2004a). Synthesis of chitosan-stabilized gold nanoparticles in the absence/presence of tripolyphosphate. *Biomacromolecules*, *5*(6), 2340–2346.

Huang, H., & Yang, X. (2004b). Synthesis of polysaccharide-stabilized gold and silver nanoparticles: A green method. *Carbohydrate Research*, *339*(15), 2627–2631.

Jiang, J., Liu, W., Cheng, J., Yang, L., Jiang, H., Bai, D., et al. (2012). A sensitive colorimetric and ratiometric fluorescent probe for mercury species in aqueous solution and living cells. *Chemical Communications*, *48*(67), 8371–8373.

Kemp, M. M., Kumar, A., Mousa, S., Park, T.-J., Ajayan, P., Kubotera, N., et al. (2009). Synthesis of gold and silver nanoparticles stabilized with glycosaminoglycans having distinctive biological activities. *Biomacromolecules*, *10*(3), 589–595.

Kumar, A., & Paul, P. (2014). Gold nanoparticles for designing of smart colorimetric logic gates operations and scavengers for mercury ions in water. *Analytical Methods*, http://dx.doi.org/10.1039/c4ay00914b

Lee, J. S., Ulmann, P. A., Han, M. S., & Mirkin, C. A. (2008). A DNA-gold nanoparticle-based colorimetric competition assay for the detection of cysteine. *Nano Letters*, *8*(2), 529–533.

Li, Y., Chen, C., Li, B., Sun, J., Wang, J., Gao, Y., et al. (2006). Elimination efficiency of different reagents for the memory effect of mercury using ICP-MS. *Journal of Analytical Atomic Spectrometry*, *21*(1), 94–96.

Lim, S., Escobedo, J. O., Lowry, M., Xu, X., & Strongin, R. (2010). Selective fluorescence detection of cysteine and *N*-terminal cysteine peptide residues. *Chemical Communications*, *46*(31), 5707–5709.

Liu, R., Chen, Z., Wang, S., Qu, C., Chen, L., & Wang, Z. (2013). Colorimetric sensing of copper(II) based on catalytic etching of gold nanoparticles. *Talanta*, *112*, 37–42.

Liu, S.-J., Nie, H.-G., Jiang, J.-H., Shen, G.-L., & Yu, R.-Q. (2009). Electrochemical sensor for mercury(II) based on conformational switch mediated by interstrand cooperative coordination. *Analytical Chemistry*, *81*(14), 5724–5730.

Lu, C., Zu, Y., & Yam, V. W.-W. (2007). Nonionic surfactant-capped gold nanoparticles as postcolumn reagents for high-performance liquid chromatography assay of low-molecular-mass biothiols. *Journal of Chromatography A*, *1163*(1–2), 328–332.

Manivannan, S., & Ramaraj, R. (2009). Core–shell Au/Ag nanoparticles embedded in silicate sol–gel network for sensor application. *Journal of Chemical Sciences*, *121*, 735–743.

Maity, D., Kumar, A., Gunupuru, R., & Paul, P. (2014). Colorimetric detection of mercury(II) in aqueous media with high selectivity using calixarene functionalized gold nanoparticles. *Colloids and Surfaces A: Physicochemical and Engineering Aspects*, *455*, 122–128.

Meena, R., Chaudhary, J. P., Agarwal, P. K., Maiti, P., Chatterjee, S., Raval, H. D., et al. (2014). Surfactant-induced coagulation of agarose from aqueous extract of *Gracilaria dura* seaweed as an energy-efficient alternative to the conventional freeze–thaw process. *RSC Advances*, *4*(53), 28093–28098.

Pal, A., Esumi, K., & Pal, T. (2005). Preparation of nanosized gold particles in a biopolymer using UV photoactivation. *Journal of Colloid and Interface Science*, *288*(2), 396–401.

Poliakoff, M., & Anastas, P. (2001). A principled stance. *Nature*, *413*, 257. http://dx.doi.org/10.1038/35095133

Radhakumary, C., & Sreenivasan, K. (2011). Gold nanoparticles generated through green route bind Hg2+ with a concomitant blue shift in plasmon absorption peak. *The Analyst*, *136*(14), 2959–2962.

Raveendran, P., Fu, J., & Wallen, S. L. (2003). Completely green synthesis and stabilization of metal nanoparticles. *Journal of the American Chemical Society*, *125*(46), 13940–13941.

Rusin, O., St Luce, N. N., Agbaria, R. A., Escobedo, J. O., Jiang, S., Warner, I. M., et al. (2003). Visual detection of cysteine and homocysteine. *Journal of the American Chemical Society*, *126*(2), 438–439.

Sandhu, K. K., McIntosh, C. M., Simard, J. M., Smith, S. W., & Rotello, V. M. (2001). Gold nanoparticle-mediated transfection of mammalian cells. *Bioconjugate Chemistry*, *13*(1), 3–6.

Spătaru, N., Sarada, B. V., Popa, E., Tryk, D. A., & Fujishima, A. (2001). Voltammetric determination of L-cysteine at conductive diamond electrodes. *Analytical Chemistry*, *73*(3), 514–519.

Taton, T. A., Mirkin, C. A., & Letsinger, R. L. (2000). Scanometric DNA array detection with nanoparticle probes. *Science*, *289*(5485), 1757–1760.

Wang, W., Rusin, O., Xu, X., Kim, K. K., Escobedo, J. O., Fakayode, S. O., et al. (2005). Detection of homocysteine and cysteine. *Journal of the American Chemical Society*, *127*(45), 15949–15958.

Wang, Z., Heon Lee, J., & Lu, Y. (2008). Highly sensitive turn-on fluorescent sensor for Hg2+ in aqueous solution based on structure-switching DNA. *Chemical Communications*, *45*, 6005–6007.

Watthanaphanit, A., Panomsuwan, G., & Saito, N. (2014). A novel one-step synthesis of gold nanoparticles in an alginate gel matrix by solution plasma sputtering. *RSC Advances*, *4*(4), 1622–1629.

Wei, X., Qi, L., Tan, J., Liu, R., & Wang, F. (2010). A colorimetric sensor for determination of cysteine by carboxymethyl cellulose-functionalized gold nanoparticles. *Analytica Chimica Acta*, *671*(1–2), 80–84.

Xue, X., Wang, F., & Liu, X. (2008). One-step, room temperature, colorimetric detection of mercury (Hg2+) using DNA/nanoparticle conjugates. *Journal of the American Chemical Society*, *130*(11), 3244–3245.

Yu, C. J., & Tseng, W. L. (2008). Colorimetric detection of mercury(II) in a high-salinity solution using gold nanoparticles capped with 3-mercaptopropionate acid and adenosine monophosphate. *Langmuir*, *24*(21), 12717–12722 (the ACS journal of surfaces and colloids).

Zhang, J., Xu, X., Yuan, Y., Yang, C., & Yang, X. (2011). A Cu@Au nanoparticle-based colorimetric competition assay for the detection of sulfide anion and cysteine. *ACS Applied Materials & Interfaces*, *3*(8), 2928–2931.